View metadata, citation and similar papers at core.ac.uk
brought to you by CORE
provided by Aston Publications Explorer

Effects in ultrafast laser micromachining PMMA-based optical fibre grating

Chen Liu[a], Xianfeng Chen*[a], Marcos R. Cardoso[b], Wei Zhang[c], David J. Webb[c]

[a]School of Electronic Engineering, Bangor University, Bangor LL57 1UT, United Kingdom
[b]Instituto de Física de São Carlos, Universidade de São Paulo, São Carlos 13560-970, Brazil
[c]Aston Institute of Photonic Technologies, Aston University, Birmingham, United Kingdom

ABSTRACT

Ultrafast laser owns extreme small beam size and high pulse intensity which enable spatial localised modification either on the surface or in the bulk of materials. Therefore, ultrafast laser has been widely used to micromachine optical fibres to alter optical structures. In order to do the precise control of the micromachining process to achieve the desired structure and modification, investigations on laser parameters control should be carried out to make better understanding of the effects in the laser micromachining process. These responses are important to laser machining, most of which are usually unknown during the process. In this work, we report the real time monitored results of the reflection of PMMA based optical fibre Bragg gratings (POFBGs) during excimer ultraviolet laser micromachining process. Photochemical and thermal effects have been observed during the process. The UV radiation was absorbed by the PMMA material, which consequently induced the modifications in both spatial structure and material properties of the POFBG. The POFBG showed a significant wavelength blue shift during laser micromachining. Part of it attributed to UV absorption converted thermal energy whilst the other did not disappear after POFBG cooling off, which attributed to UV induced photodegradation in POF.

Keywords: Bragg grating, polymer optical fibre, PMMA, photodegradation.

1. INTRODUCTION

The polymeric materials have very different physical and chemical properties to silica, which make them attractive for research to exploit in device and sensing applications. Polymer optical fibres (POFs) provide additional advantages for sensing applications, including high strain limits, high fracture toughness, high flexibility in bending, large negative thermo-optic coefficients and for some materials an affinity for water. Polymers have excellent compatibility with organic materials, giving them great potential for biomedical applications [1]. Over the last decades, fibre Bragg grating (FBG) technology has been extensively developed to inscribe Bragg gratings in step-index [2] and microstructured optical polymer fibres (mPOFs) made of poly(methyl methacrylate) (PMMA) materials, TOPAS, and polystyrene polymer [2-7]. Since the first FBG successfully inscribed in polymer optical fibre [2], extensive research have been carried on PMMA-based optical fibre Bragg gratings (POFBGs). With the unique properties, POFBGs have been found to be sensitive to relative humidity, temperature, strain and pressure with high sensitivity [8-11]. Recent investigations present that the POFBG sensing performance can be improved by reducing the fibre diameter with chemical etching as well as by using laser micromachining [9, 12].

The ultrafast laser owns extreme small beam size and high pulse intensity, which provide an effective technique to enable spatial localised in materials inducing permanent changes on the surface or into the bulk of materials. Excimer laser can produce light in deep UV region of the spectrum and most polymer materials will absorb such radiation. Hence excimer laser micromachining has been used as an interesting approach to process polymeric materials. Laser micromachining occurs when the laser beam acts on a material and its molecular bonds are broken by the absorption of the UV photons. The mechanism of FBG inscribed in polymer fibre is the photoinduced refractive index change effect in the polymer materials. However, it is still not fully clear that the UV radiation induced photosensitivity effects in PMMA material [13-16].

* x.chen@bangor.ac.uk ; phone 44 1248 382480; fax 44 1248 361429

Micro-Structured and Specialty Optical Fibres IV, edited by Kyriacos Kalli, Alexis Mendez, Proc. of SPIE Vol. 9886, 98861O · © 2016 SPIE
CCC code: 0277-786X/16/$18 · doi: 10.1117/12.2230230

In order to obtain the desired structure, laser parameters such as energy, repetition, and number of pulses need to be precisely controlled. These parameters are designed based on the knowledge of materials to be machined. The response of materials to the laser pulse will depend on the optical absorption and the photochemical, thermal and mechanical effects. When micromachining POFBG these effects can be observed by monitoring the Bragg reflection of POFBG which shows interesting features under different laser machining conditions.

In this work, we used laser micromachining technology associated with fibre grating technique to investigate the photosensitive mechanism of polymer fibre. This work gets insight of laser micromaching material performance of polymer optical fibres, revealing the comprehension properties may depend on different mechanisms.

2. PRINCIPLE AND POFBG FABRICATION

POFBG wavelength depends on the effective index of the fibre core n_{co}^{eff} and the grating pitch Λ. For the polymer FBG, both of which are the function of temperature T and the water content w. Hence the Bragg wavelength can be expressed as [9]

$$\lambda_B = 2n_{co}^{eff}(T,w)\Lambda(T,w) \tag{1}$$

For the constant relative humidity, the wavelength changes only against temperature

$$\Delta\lambda_B = \lambda_B(\alpha+\xi)\Delta T \tag{2}$$

where α is the thermal expansion coefficient related to the volumetric change induced by thermal effect, and ξ is the normalised thermo-optic coefficient which describes the refractive index as a function of temperature. It is well known that the thermo-optic coefficient of PMMA is negative, so the heat introduced negative refractive index change of fibre core is dominant the Bragg wavelength shift.

The FBG was fabricated in PMMA-based fibre by the phase mask technique using the UV laser with an output wavelength of 325 nm. A short length of 7 cm POF was used to inscription of a POFBG as the high transmission loss of POF in the 1550 nm wavelength region. The POF was mounted horizontally in a v-groove, the laser beam was focused vertically down on the fibre axis using a cylindrical lens of focal length 10 cm. A phase mask with period of 1.038 μm was placed on top of the POF to generate a periodic refractive index modulation in fibre core. The laser beam was scanned 5 mm along the phase mask. The spectrum shown in Fig. 1, reveals a triple peak corresponding few modes due to the increase of fibre diameter during POF pre-treated annealing process (at 80°C, over 7 hours).

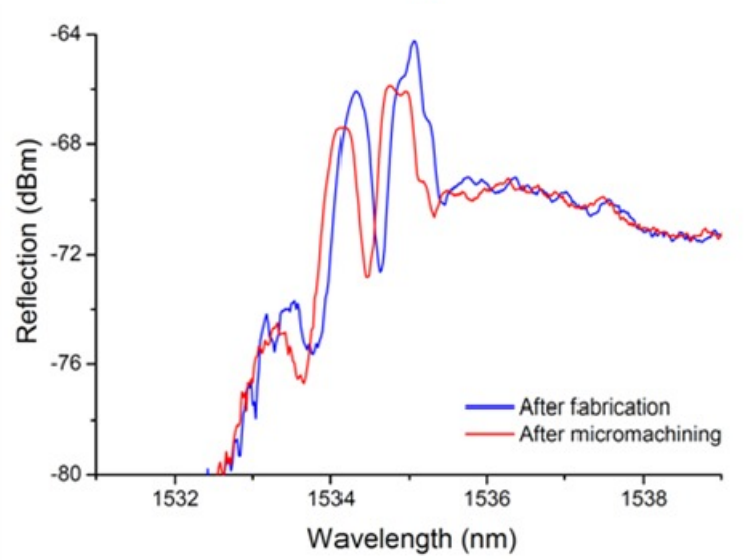

Fig. 1. Reflection spectra of POFBG after fabrication (blue line) and after laser micromachining (red line).

3. LASER MICROMACHINING OF POFBG

As most polymer materials absorbed deep UV radiation, the excimer laser with 248 nm UV beam was chosen for the micromachining. Fig. 2 illustrates the laser micromachining system and the real-time optical measurement system. The excimer laser system (Exitech Ltd Oxford, UK) produced a 248 nm KrF laser beam and contains XY mask stage and a high precision air-bearing work piece handling stage. The laser beam was homogenized to produce a uniform intensity profile at the mask plan. After the fly's eye homogenizer, the laser beam profile became a 1 cm×1 cm square with relatively uniform beam front and projected the open square aperture (2 mm×2 mm mask) through a projection lens (with a demagnification of ×10) forming a 200 μm×200 μm square image onto the polymer FBG sample, which was fixed on a micro-positioning work piece stage. The projection of focused laser beam had larger size (200 μm) than POFBG outer diameter (130 μm) hence to create a D-shaped structure on fibre cladding whereas FBG underneath by moving grating sample along the fibre axial direction.

The PMMA-based POF contained a 5 mm long FBG was connected to a single mode silica fibre down-lead using UV curable glue (Norland 76). The POFBG was launched via a 3-dB coupler with light from a broadband source and the spectrum was monitored by using an optical spectrum analyzer (OSA, HP86142) during the laser micromachining process.

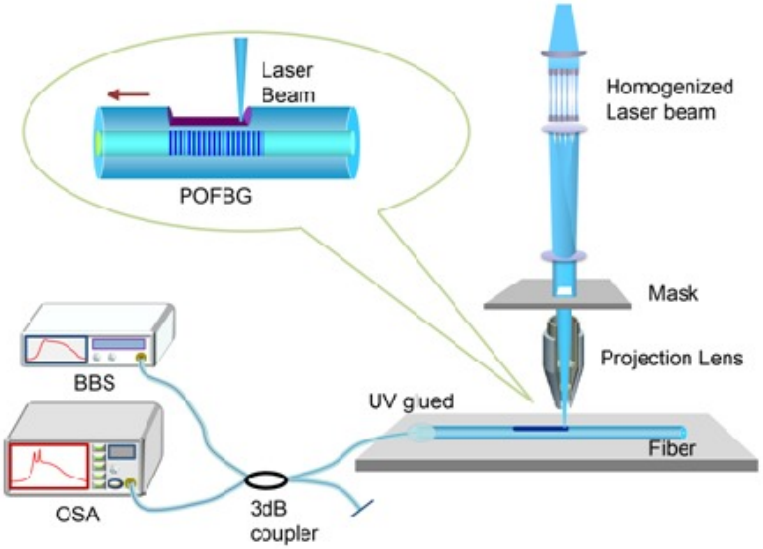

Fig. 2. Schematic of the excimer laser micromachining system and optical measurement system.

4. POFBG SPECTRAL EVOLUTION UNDER LASER MICROMACHINING

During the laser micromaching process, the grating reflection spectra were captured when the laser beam was projected onto the grating region at start point of 0 mm (laser off, curve A), process points of 1 mm, 2 mm, 3 mm, and 4 mm (laser on, curve B to E), and the final point of 5 mm (laser off, curve F), respectively. All the curves are plotted in Fig. 3 (with offset).

For the whole micromachining process, the grating spectra showed not only the wavelength shift but also the peak splitting and reunion characteristics. Initially, curve A showed the multi-peaks at 1535.2 nm, 1534.3 nm and 1533.2 nm indicating the few-moded feature of POFBG after bare POF pre-treated annealing process and FBG inscription. When the laser beam started to fire on the POFBG (curve A to B), the grating resonances immediately moved to the short wavelength side, whereas the peak splitting appeared simultaneously. During laser firing, all Bragg peaks were keeping blue shift (curve B to E) until the laser was off (curve F) at which the split-subpeaks merged again then moved towards long wavelength side when the POFBG was cooling down eventually.

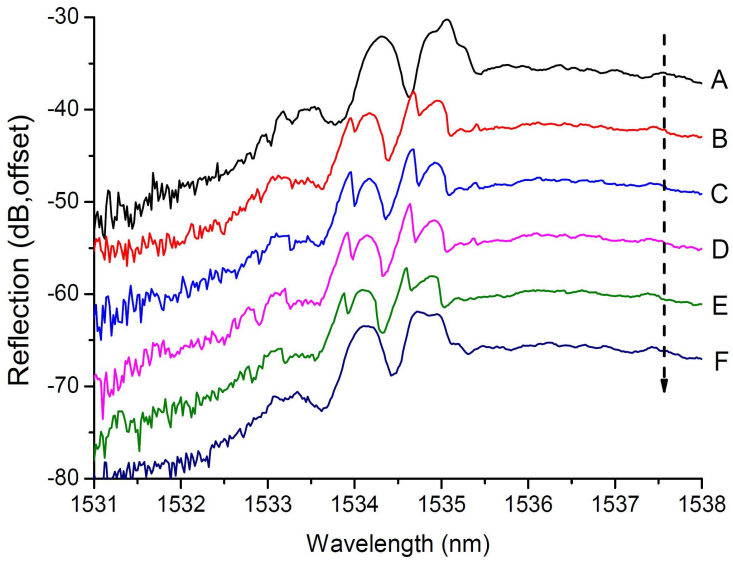

Fig. 3. POFBG spectral evolution during laser micromachining.

The Bragg peak at 1534.3 nm was selected for detail analysis. Fig. 4 plots Bragg resonance features of splitting, merging and movement. The light blue area in Fig. 4 indicates the laser beam was switched on and was scanning along the POFBG region. When the laser beam was projected onto POFBG, the Bragg peak split into two subpeaks immediately (just after the start point A), then they were keeping blue shift with a nearly constant wavelength separation of 220pm. When the laser was off (point F), the split-subpeaks were reunion and moved towards long wavelength side during POFBG cooling down process. The total wavelength change caused laser micromachining (point A and F, both at room temperature) is -180 pm.

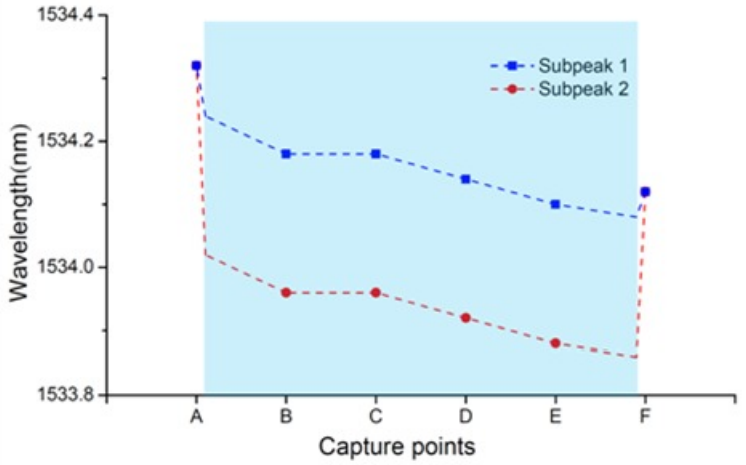

Fig. 4 Peak-splitting feature of Bragg resonance under laser scanning.

The spectral characteristics of POFBG under laser micromachining are more complex, which may be explained by the modulation of core refractive index profiles during machining [17, 18]. The UV laser resulted in two major effects in POFBG including the thermal effect caused by the absorption of UV radiation as well as the UV induced photodegradation [19, 20].

When 248 nm UV beam was focused onto POFBG sample, the heat was generated and distributed to the entire grating region immediately. From Eq. (2), the heat made the contributions in both thermal expansion and thermo-optic effect, where the thermal expansion tended to increase Bragg wavelength whilst the negative thermo-optic factor made a dominant contribution resulting a mean refractive index decrease of fibre core, hence the blue wavelength shift. Moreover, the laser beam projected onto the POFBG was around 200 μm in width, which was 1/25th of the grating length (5 mm). When the laser beam was firing along the POFBG, the mean refractive index profile of POFBG was splitting into two regions (micromachined and un-machined POFBG) leading into two sub-gratings and hence two subpeaks. Comparison with its counterpart, the micromachined-POFBG absorbed strong UV irradiation yielding a further photoinduced refractive index decrease. As a consequence of photodegradation, the decrease in refractive index of ~ 2.1×10^{-4} resulted in two sub-gratings, therefore two subpeaks with 220 pm separation accordingly. During laser firing, all peaks were keeping blue shift were due to the further decrease of refractive index induced by the accumulated heat. After the whole region of POFBG was micromachined, the split index profiles were reunion hence two subpeaks merged again. All the Bragg peaks moved to long wavelength side after laser beam switched off (heating source removed) and the POFBG was cooled down to room temperature.

5. CONCLUSION

In this work, we presented the investigation of spectral characteristics of PMMA-based fibre Bragg grating under excimer laser micromachining. The unique spectral evaluation was observed with the features of peak shift, splitting and reunion which have different mechanisms. Under laser firing, the negative thermal-optic factor in POF made a dominant contribution resulting POFG mean refractive index decrease, hence the negative wavelength shift. The peak splitting and reunion properties indicated that the mean refractive index profile of POFBG was modulated yielding two sub-gratings by different UV absorption between micromachined and un-machined POFBG regions. In which, the main photosensitive mechanism is the consequence of the photodegradation.

6. ACKNOWLEDGEMENTS

This work was supported by Marie Curie Scheme included in the 7th Framework Programme of the European Union (FP7 PIRSES-2013-612267, iPhoto-Bio). The authors also would like to acknowledge the support from the Sêr Cymru NRN097.

REFERENCES

[1] Webb, D. J. and Kalli, K., Polymer fiber Bragg gratings, in *Fiber Bragg Grating Sensors*, A. Cusano, A. Cutolo, and J. Albert Eds. Oak Park, IL, USA: Bentham Science Pub., 292-312, (2011).

[2] Xiong, Z., Peng, G.-D., Wu, B. and Chu, P. L., "Highly tunable Bragg gratings in single-mode polymer optical fibers," IEEE Photon. Technol. Lett., 11(3), 352-354, (1999).

[3] Dobb, H., Webb, D. J., Kalli, K., Argyros, A. Large, M. C. J. and van Eijkelenborg, M. A. "Continuous wave ultraviolet light-induced fiber Bragg gratings in few- and single-mode microstructured polymer optical fibers," *Opt. Lett.*, 30(24), 3296-3298, (2005).

[4] Carroll, K. E., Zhang, C., Webb, D. J., Kalli, K., Argyros, A. and Large, M. C. J. "Thermal response of Bragg gratings in PMMA microstructured optical fibers," *Opt. Express*, vol. 15(14), 8844-8850, (2007).

[5] Bundalo, I. L., Nielsen, K., Markos, C. and Bang, O., "Bragg grating writing in PMMA microstructured polymer optical fibers in less than 7 minutes," *Opt. express*, 22(5), 5270-5276, (2014).

[6] Yuan, W., Khan, L., Webb, D. J., Kalli, K., Rasmussen, H. K., Stefani, A. and Bang, O., "Humidity insensitive TOPAS polymer fiber Bragg grating sensor," *Opt. Express,* 19(20), 19731-19739, (2011).

[7] Harbach, N. G., "Fiber Bragg gratings in polymer optical fibers," PhD Thesis, Lausanne, EPFL, (2008).

[8] Zhang, W. and Webb, D. J., "Humidity responsivity of poly (methyl methacrylate)-based optical fiber Bragg grating sensors," *Opt. Lett.*, 39(10), 3026-3029, (2014).

[9] Zhang, W., Webb, D. J. and G.-D. Peng, "Investigation into time response of polymer fiber Bragg grating based humidity sensors," *J. Lightw. Technol.*, 30(8), 1090-1096, (2012).

[10] Chen, X., Zhang, C., Webb, D. J., Kyriacos, K. and Peng, G.-D., "Highly sensitive bend sensor based on Bragg grating in eccentric core polymer fiber," *IEEE Photon. Technol. Lett.*, 22(11), 850-852, (2010).

[11] Bhowmik, K., Peng, G-D, Luo, Y., Ambikairajah, E., Lovric, V., Walsh, W. R. and Rajan, G., "Experimental study and analysis of hydrostatic pressure sensitivity of polymer fiber Bragg gratings," *J. Lightw. Technol.*, 33(12), 2456-2462, (2015).
[12] Chen, X., Zhang, W., Liu, C., Hong, Y. and Webb, D. J., "Enhancing the humidity response time of polymer optical fiber Bragg grating by using laser micromachining," *Opt. Express*, 23(20), 25942-25949, (2015).
[13] Liu, H. Y., Peng, G.-D. and Chu, P. L., "Thermal tuning of polymer optical fiber Bragg gratings," *IEEE Photon. Technol. Lett.*, 13(8), 824-826, (2001).
[14] Baker, A. K. and Dyer, P. E. "Refractive-index modification of polymethylmethacrylate (PMMA) thin films by KrF-laser irradiation," *Appl. Phys. A*, vol. 57, no .6, 543-544, (1993).
[15] Holmes, A. S., "Excimer laser micromachining with half-tone masks for the fabrication of 3-D microstructures," *Science, Measurement and Technology*, IEE Proceedings, 151, IET, (2004).
[16] Burt, J., Goater, A., Menachery, A., Pethig, R., and Rizvi, N., "Development of microtitre plates for electrokinetic assays," *J. Micromech. Microeng.,* 17, 250-257, (2007).
[17] Simpson, G., Kalli, K., Zhou, K., Zhang, L. and Bennion, I., "Formation of type IA fibre Bragg gratings in germanosilicate optical fibre," *Electron. Lett.*, 40(3), 163-164, (2004).
[18] Simpson, G., Kalli, K., Zhou, K., Zhang, L. and Bennion, I., "Blank beam fabrication of regenerated type IA gratings," *Meas. Sci. Technol*., 15(8), 1665-1669, (2004).
[19] Sáez-Rodríguez, D., Nielsen, K., Bang, O., and Webb, D. J., "Photosensitivity mechanism of undoped poly (methyl methacrylate) under UV radiation at 325 nm and its spatial resolution limit," *Opt. Lett*., vol. 39, no. 12, pp. 3421-3424, (2014).
[20] Oliveira, R., Bilro, L., and Nogueira, R., "Bragg gratings in a few mode microstructured polymer optical fiber in less than 30 seconds," *Opt. express*, vol. 23, no .8, pp. 10181-10187, (2015).